⊙ 速報硏究論文

A Study on the Heat and Mass Transfer Characteristics of Vacuum Freeze Drying Process for Porous Media

C-S Song*

다공성 물질의 진공동결건조과정에서 열 및 물질전달 특성에 관한 연구

송 치 성

Key words : Freeze drying(동결건조), Heat & Mass Transfer(열 및 물질전달), Porous Media(다공성 물질), Eutectic point(공융점), Finite Volume Method(유한 체적법), Moving grid system(이동격자계)

Abstract

Vacuum freeze drying process by which frozen water in a drying material is removed sublimation under vacuum condition, is now applied to various industrial field such as the manufacturing and packaging of pharmaceuticals in pharmaceutical industry, the drying of bio-products in bio-technology industry, the treatment of various quality food stuff in food technology, and so on.

The knowledge about the heat and mass transfer characteristics related with the vacuum freeze drying process is crucial to improve the efficiency of the process as well as the quality of dried products. In spite of increasing needs for understanding of the process, the research efforts in this fields are still insufficient.

In this paper, a numerical code that can predict primary drying in a vial is developed based on the finite volume method with a moving grid system. The calculation program can handle the axis-symmetric and multi-dimensional characteristics of heat and mass transfer of the vial freeze drying process.

To demonstrated the usefulness of the present analysis, a practical freeze drying of skim milk solution in a vial is simulated and various calculation results are presented.

* Korea Institute of Machinery and Materials(KIMM), PO Box 101, Yusong, Taejon 305-600, Korea, e-mail address : scs1675@mailgw.kimm.re.kr

Nomenclature.

A : Area [m^2]
C : Weight fraction of bound water in dried layer [kg water/kg solid]
C_p: Specific heat [J/kg-K]
D : Diameter [m] or diffusion coefficient [m^2/s]
h : Position of sublimation interface [m]
h' : Enthalpy [J/kg]
K : Thermal conductivity [W/m-K]
K_n: Knudsen number
M : Molecular weight [kg/kmol]
N : Mass flux in dried layer [kg/m^2-s]
P : Total pressure in dried layer or pressure [N/m^2]
Q : Heat flux [W/m^2]
T : Temperature [K]
X : Position of 1-dimensional sublimation interface [m]
ΔH_s:Heat of sublimation of frozen water [J/kg]
ΔH_v:Heat of vaporization of sorbed water [J/kg]
ε : Void fraction
μ_{mix}: Mixture viscosity of water vapor and inert gas [kg/m-s]
λ : Mean free path [kg/m^3]
τ : Totyuosity of porous media
ρ : Density [kg/m^3]
σ : Stefan-Boltzmann constant [W/m^2K^4]

1. Introduction.

Freeze dying is a process by which frozen free water in drying materials is removed by sublimation under vacuum condition. The use of relatively low temperature and vacuum pressure in the freeze drying minimizes the thermal and chemical degradation. And the volatile aroma components and the original porous structures of the drying material are largely retained.

In spite of the merits of freeze drying, its practical use is restricted to the drying of relatively high-quality and high-price products such as pharmaceuticals, bio-products, and so on for its high operation cost such as time cost, labor cost and energy cost. Thus, there has been much numerical and experimental effort to enhance the productivity by minimizing drying time and energy consumption without major loss of quality through the optimal operation policies. As the operation times required for pre-freezing and secondary drying is relatively insensitive to the operation conditions, the reduction of primary drying time is the most efficient ways to reduce overall drying time.

In a pharmaceutical industry, many products are freeze-dried in cylindrical containers such as vials. For the accurate prediction of the process, multi-dimensional effects such as energy inflow from the sidewall of a vial, the deformation of sublimation interface or ice front, etc. should be properly handled. The researches on the multi-dimensional freeze drying in vial have been published rather recently. For the discretization of 2-dimensional the governing equations, either finite difference method ([6]Sheehan and Liapis, 1998; [7]Sadikoglu and Liapis, 1997; [8]Sadikoglu et al. 1999) or finite element method ([5]Mascarenhas et. al. 1998) was used with sorption-sublimation model of [9]Liapis and Litchfield (1979), which is known to produce the most accurate results.

The numerical analysis based on finite volume method is seldom tried for the analysis of multi-dimensional freeze drying in a vial in spite of its numerical advantages. Only in the context of freeze drying of foodstuffs, the finite volume method was used ([4]Lombrana et. al., 1997; [10]Wang and Shi, 1998), but their calculation model is different from the

sorption-sublimation model. The finite volume method is a conservative method that ensures strict conservation of energy and mass, and the discretization of the governing equations by the method is much easier to understand than that by the finite difference method.

Therefore, we develop a numerical procedure for the analysis of the freeze drying in vials with a finite volume method and a moving grid system. And skim milk solution, which well simulates the various pharmaceutical products, is selected as an objective drying material because its properties are documented.

2. Problem Statement.

A configuration of a vial placed on the heating plate, and a schematic of the process considered in this study are shown in Fig. 1. The dried and frozen region in the drying material is divided by a curved sublimation interface in this case. At the start of the primary dying stage, there exists only a frozen region and the initial position of sublimation interface is written as h(r,t = 0) = L.

During the primary drying stage, the material is dried or dehydrated by sublimation of frozen ice below the triple point of water and the vapor generated by the sublimation is exhausted from the drying material. As the sublimation goes on, the thickness of the dried layer increases and sublimation interface backs away from its initial position toward the bottom of the vial. When the sublimation interface reaches the bottom of the vial and the frozen region disappears, the primary drying is terminated and the secondary drying is initiated.

For freeze drying process in a vial, the heat transferred through the sidewall is considerable and this heat produce curvature of

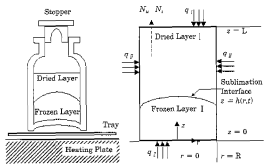

Fig. 1: A schematic of a freeze drying process in a vial

the sublimation interface. The quantities q_l, $q_{\bar{s}}$, and $q_{\bar{s}}$ shown in Fig. 1 represent the heat fluxes at top, bottom and side surfaces of a vial, respectively. Generally, q_l is delivered from an upper heating plate down to the top surface by radiation. Likewise, $q_{\bar{s}}$ is delivered to the bottom surface by radiation and conduction. The heat flux at the sidewall, $q_{\bar{s}}$, is a combination of the radiation from upper heating plate, lower heating plate, and the walls of a drying chamber, and conduction through the wall of the vial. In general, $q_{\bar{s}}$ is greatly affected by the position and the arrangement of vials (Sheehan and Liapis, 1998).

In Fig. 1, N_w and N_i represent mass fluxes of water vapor and inert gas, respectively, and N_t the total mass flux summing N_w and N_i. Here, the terms that are not bold-typed mean the mass flowrates through a surface, that is, dot products with respect to the unit normal vector of the surface.

3. Mathematical Formulation.

From the conservation of energy, the governing equations for heat transfer are obtained as follows. The different forms in the dried and frozen regions are the results of their different heat transfer characteristic. The

Eq.(1) is for the dried region and Eq.(2) for the frozen region.

$$\rho_{ie}C_{ie}\frac{\partial T_i}{\partial t}+\nabla\cdot(N_iC_{pg}T_i-K_{ie}\nabla T_i)=\Delta H_s\rho_i\frac{\partial C}{\partial t} \quad (1)$$

$$\rho_{fe}C_{pfe}\frac{\partial T_{ff}}{\partial t}+\nabla\cdot(-K_{fe}\nabla T_{ff})=0 \quad (2)$$

The last term in Eq.(1) represents the latent heat source by vaporization of bound water. The initial and boundary conditions for heat transfer are given as follows.

$$T_i=T_{ff}=T_X=T^0 \quad (3)$$

$$q_i=\sigma F_{UP}(T_{UP}^4-T_{z=L}^4) \quad (4)$$

$$q_f=k_f(T_{LP}-T_{z=0}) \quad (5)$$

$$q_i=h_o(Tw-T_{r=R}) \quad (6)$$

Above boundary conditions are derived considering the radiation in the upper surface, the radiation and conduction in bottom and side surfaces. Here, F is shape factor for radiation calculation, K_f film heat transfer coefficient of bottom surface.T_{UP} , T_{LP} and T_W are the temperatures of the upper and lower heating plates and that of walls of freeze dryer, respectively. For general freezing dryers, the temperatures of the upper and lower heating plates are same but the temperature of the walls of a freeze dryer, T_W, is around ambient temperature because of heat transfer through freeze dryer walls. The boundary condition at the centerline of a vial (r = 0) is not given because a symmetry condition is sufficient for this condition.

At this time, to complete the governing equations for heat transfer, a governing equation for the behavior of the sublimation interface is required. From the conservation of mass and energy at the sublimation interface, the following equation is derived.

$$A_i\cdot[-k\nabla T-V_bC_pT]_{z=h^-}^{z=h^+}N_wC_{pg}T_X+\Delta H_sN_w=0 \quad (7a)$$

In Eq.(7a), A_i is a surface normal vector of the sublimation interface directing from the frozen region toward the dried region. If we rewrite Eq.(7a) using the coordinates shown in Fig. 1, the following equation results.

$$A_i\cdot(k_i\nabla T_i-k_{ie}\nabla T_i+V\rho_iC_{pi}T_i-V\rho_iC_{pi}T_i)$$
$$+N_wC_{pg}T_X+\Delta H_sN_w=0 \quad (7b)$$

Here the velocity of sublimation interface,V, in Eq.(7a) and Eq.(7b) is a vector whose magnitude is defined as follows.

$$|V|=\frac{N_w}{\rho_i-\rho_i}=\frac{dh}{dt} \quad (8)$$

For most practical freeze drying processes, the effect of inert gas is negligible because the amount of inert gas in the drying chamber is much smaller than that of water vapor. Thus the mass flux calculation of inert gas is eliminated without loss of generality of this study.

$$\varepsilon\frac{M_w}{R}\frac{\partial}{\partial t}\left(\frac{P_w}{T_i}\right)=-\nabla\cdot N_w\rho_i\frac{\partial C}{\partial t} \quad (9)$$

$$\frac{\partial C}{\partial t}=-k_dC \quad (10)$$

The Eq.(9) is a so-called continuity equation that explains the conservation of water vapor and the last term is the mass source term by the vapor generation. The governing equation for the removal of bound water, Eq.(10), shows an empirical relationship that the rate of bound water removal is proportional to its *content in the material*. To complete Eq.(9), we need a constitute equations for N_w. In the original sorption-sublimation model, the consititutive equations for mass transfer were based on the dusty-gas model. But the three empirical constants in the dusty-gas model are hard to ditermine. Thus, the consititutive equation that is derived by effective mass transfer concept is adopted in this study as in Eq.(11). This approach is proved to be advatageous in practical use because only one empirical constant need to be determined.

$$N_w=-\frac{M_w}{RT_i}\left(D_e\nabla P_w\right) \quad (11)$$

Equation (11) constitutes the governing equation of vapor pressure when substituted in Eq.(9). The initial and boundary conditions for vapor pressures and concentration of bound water are as follows.

$$P_w = P_w^o,\ C = C^o \tag{12}$$
$$P_w = P_{w^i}^o \text{; for } z = L \tag{13}$$
$$P_w = f(T_s),\ \text{for } z = h\ (r,t) \tag{14}$$
$$N_w = 0,\ \text{for } z = 0 \tag{15}$$

The pressure boundary condition at the top surface of drying material is defined as a constant pressure inside the drying chamber and the vapor pressure at the sublimation interface is defined as an equilibrium vapor pressure according to the temperature of the interface. The conditions for all walls of a vial and at centerline ($r = 0$) are given as zero mass fluxes same as Eq.(15).

4. Discretization Method.

Freeze drying process is a typical moving boundary problem with moving boundaries and change in the computational domains. There are two solution methods for these kinds of problems; fixed grid analysis and moving grid analysis. When the deformations of the boundaries are small, the moving grid analysis is more efficient and accurate. To analyze the freeze drying process in vials using a finite volume method with a moving grid system, we should be able to adequately treat problems resulting from the movement of grid system. The first problem is non-orthogonality of grid system by the movement of grids, and that is handled by introducing the finite concept of spatial gradient (2)Kim, 2000) as shown in Fig. 2.In the non-orthogonal coordinates system, the diffusion flux of a general scalar variable through a control surface of a control volume

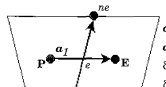

$$\nabla\phi \doteq \frac{(\delta A)_i(\delta\phi)_i}{(\delta V)}$$

Fig. 2: A diagram for the illustration of the finite concept of spatial gradient of a scalar quantity

can be defined as follows, for an east face.

$$J_e^o = \delta A_e \cdot (-\Gamma_e \nabla\phi) \tag{16}$$

Here, the superscript and the subscript denote the diffusion and east face, respectively. And the terms δA_e and Γ_e denote surface normal vector of east face and the diffusion coefficient of the scalar. By introducing finite concept of spatial gradient of ϕ shown in Fig. 2, Eq.(16) can be rewritten as follows.

$$J_e^o = \delta A_e \cdot \left(-\Gamma_e \frac{\delta A_e}{\delta V_e}(\phi_E - \phi_P) - \Gamma_e \frac{\delta A_n}{\delta V_e}(\phi_{ne} - \phi_{se})\right)$$
$$\Gamma_e = \frac{\delta A_e \cdot \delta A_n}{\delta V_e}(\phi_P - \phi_E) - \Gamma_e \frac{\delta A_e \cdot \delta A_n}{\delta V_e}(\phi_{ne} - \phi_{se})$$
$$= \alpha_e(\phi_P - \phi_E) - s_e^{nn} \tag{17}$$

In the above equation, A_e and s_e^{nn} are the diffusion coefficient and heat generation term that accounts for the secondary diffusion due to the non-orthogonality of the grid system, respectively. Equation (17) are applied equally to all control surfaces of a control volume, say east, west, north and south faces.

The second problem is the inflow of energy and mass through moving control surfaces. Figure 3 shows a typical moving control volume. Squares drawn by solid and dashed lines represent the positions and shapes of a control volume at time t^* and at time $t^* + \Delta t$, respectively. Superscript o means the values at time t, and v_e is moving velocity of east control surface. The shaded portion, S_s, is sweeping

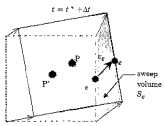

Fig. 3: The definition of sweep volume of east face of a moving two-dimensional control volume

volume (Ferziger and Peric, 1996) by movement of the east face and defined positive when it moves outward with respect to the control volume. For general scalar ϕ, in case of no diffusion, convection and generation terms, the sweeping volume that flows into control volume can be obtained as Eq.(18).

$$\frac{\phi_P \Delta V - \phi_P^o \Delta V^o}{\Delta t} = \sum_{i=e,w,n,s} \frac{S_i \phi_i}{\Delta t} \tag{18}$$

After all, ϕ_P in Eq.(18) is a Lagrangian variable that represent the state of the moving control volume. Therefore the scalar inflow terms obtained by the above relation must be added to meet the conservation of energy or mass.

5. Numerical Procedure.

The overall calculation steps are as follows. First, the temperature fields of the dried and frozen regions are obtained by solving the governing equations for heat transfer, that is Eq.(1) ~Eq.(8). And then, the pressure field and bound water concentration field in the dried region are analyzed with Eq.(9) ~ Eq. (15). After the calculation, the position of sublimation interface is determined by Eq.(8) to meet the mass conservation. These calculations are repeated until all the variables, those are temperature, pressure, sorbed water concentration and interface position, converge to a given level of accuracy, 10^{-2}. Then the above procedures are repeated for each time step with increment in time until the calculation time reaches the prescribed end time.

At the beginning of the analysis, the initial thickness of the dried region is set to 0.005 of the total thickness of the drying material. When the thickness of frozen layer becomes smaller than 0.005 of the total thickness, the primary drying analysis is terminated. A equally spaced 10×10 grid is used for each dried and frozen region, which is sufficient to capture the multi-dimensional effects of the process.

For temporal discretization, the first order implicit method is used. To ensure the stability of calculation at the beginning of analysis, the initial time step is set to sufficiently small value, 10^{-3}. But later it is automatically adjusted for the control surface to move less than 1% of the length of each control volume for each time step in a program. In order to handle non-linearity due to the movement of the sublimation interface, an iterative calculation is needed and a successive substitution method is used with under-relaxation. The discretized algebraic equations for temperature and pressure are solved using a bi-conjugate gradient solver.

5-1. Results.

In this study, a realistic freeze drying processes is simulated to show the ability of the present numerical program. The required boundary conditions and properties of skim milk solution are listed in Table 1. First, the mass reduction results are presented in Fig. 4. The figure shows that the primary drying stage ends around 12 hours and at that time about 84% of initial mass is removed by the sublimation. During the primary drying stage, the drying rate is almost constant but slightly decreases according to

Table 1: The parameters and properties for analysis of freeze drying of skim milk in vials

Parameters	Unit	Values	Parameters	Unit	Values
L	m	0.0165	h_f	W/m · K	90
R	m	0.0095	h_c	W/m · K	12
ε		0.706	F_{UP}		1.0
D_e	m²/s	0.012	C^*	kg water /kg solid	0.6415
ρ_{ie}	kg/m³	145.0			
ρ_s	kg/m³	1050.0	k_d	1/s	6.48×10^{-7}
C_{pg}	J/kg · K	1616.6			7.08×10^{-5}
Cp_{ie}	J/kg · K	2590.	T^*	K	258.15
Cp_s	J/kg · K	1930.	T_{UP}, T_{LP}	K	263.15
ΔH_s	J/kg	2840000.	T_W	K	263.15
Δh_v	J/kg	2687400.	P_0	N/m²	97.3
k_{ie}	W/m · K	0.01	P^*_{in}, P_{in0}	N/m²	4.0
k_s	W/m · K	2.1	P^*_w, P_{w0}	N/m²	93.3

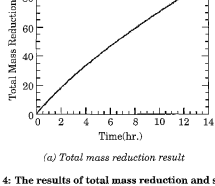

(a) Total mass reduction result

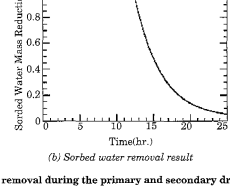

(b) Sorbed water removal result

Fig. 4: The results of total mass reduction and sorbed water removal during the primary and secondary drying

time. In addition, it is observed that the removal of bound water during the primary drying is almost negligible.

Figure 5 shows the history of temperature at the sublimation interface during the primary drying stage. The temperature history shows the temperature at sublimation interface has some range. This phenomenon is unique to multi-dimensional freeze drying different from 1-dimensional one and heat transfer through sidewall, difference in interface velocity, distribution of mass transfer resistance, etc. are responsible for the phenomenon. In general, the interface temperature continuously increase with time, which is well explained as the resistance to mass transfer increases with increase of thickness of the dried region. When the mass transfer resistance increases, a higher interface pressure is required to exhaust the same amount of water vapor.

The energy transferred through each surface of a vial is plotted in Fig. 6. The dominant energy source for sublimation is the energy from the bottom heating plate for the present simulation. But at certain conditions, the heat through the sidewall can be dominant.

If we monitor the temperatures at fixed points, the temperature histories in Fig. 7 can be obtained. Each temperature history in Fig. 7

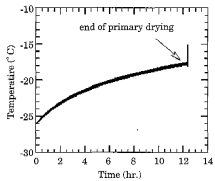

Fig. 5: The temperature history of the sublimation interface during the primary drying

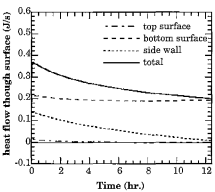

Fig. 6: The history of heat flow through the surfaces of a vial during the primary drying

shows an abrupt increase of temperature at some time and the time becomes later and later as the depth of monitoring position increases. The time of abrupt temperature change corresponds to the instance at which sublimation interface passes the monitoring position. When the fixed point belongs to the frozen region, relatively low temperature of the frozen region is maintained. But when the point belongs to the dried region, the temperature increases rapidly due to the low thermal conductivity of the dried region. In Fig. 6 the temperature near the sidewall of a vial is more rapidly increases than other two temperature histories (centerline and r = 4mm) by the effect of heat transfer through

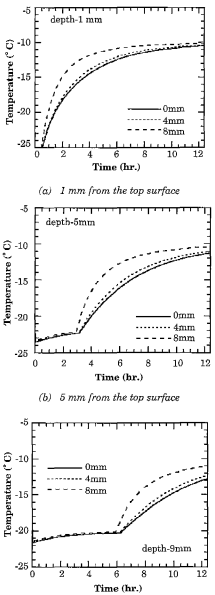

Fig. 7: The temperature histories at several fixed points during the primary drying

sidewall.

In Fig. 8 the calculated temperature distributions inside a vial at different times are presented. While the temperature distribution in the frozen region is almost 1-dimensional,

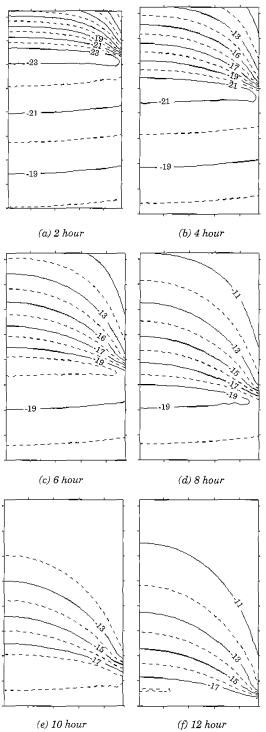

Fig. 8: The temperature distribution inside a vial during the primary drying

that in the dried region shows much distortion by the heat transfer from the sidewall of vial. But as the thermal conductivity of the dried region is two orders of magnitude smaller than that of the frozen layer, the distortion of temperature distribution in the dried region does not have much effect on the deformation of the sublimation interface.

Figure 9 shows the configurations of the calculated sublimation interfaces at the interval of one hour. In the figure, the configuration of interface is rather flat throughout the process, but the curvature of the interface becomes larger according to the

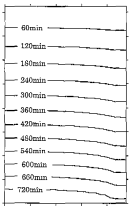

Fig. 9: The configurations of sublimation interface during the primary drying

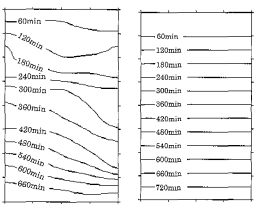

(a) by temperature (b) by mass reduction

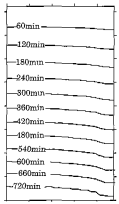

(c) by calculation

Fig. 10 The comparison of the position of the sublimation interface between numerical and experimental results.

process. And the sublimation near the sidewall is generally faster than that in the centerline.

Fig. 10 shows the calculated and estimated configurations of the sublimation interfaces at the interval of one hour. When a measured temperature history at a position shows a steep increase at a certain time, then that time is when the sublimation interface passes that position. From this consideration, the measure temperature histories can be used to estimate the sublimation interface. But as the temperature measurement is done every 20 minutes, the sublimation interface obtained by temperature history data gives only qualitative results. In the figure, (a) is the estimated from the temperature histories, (b) from the mass reduction results, and (c) is the calculated result. The estimated sublimation interface from the mass reduction is 1-dimensional, while that from the temperature histories are very distorted. The calculated configuration of sublimation interface is rather flat throughout the process, but the curvature of the interface becomes larger according to the process. And the sublimation near the side-wall is generally

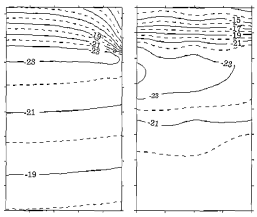

calculation experiment

(a) 2 hr.

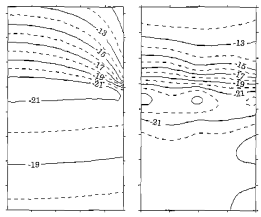

calculation experiment

(b) 4 hr.

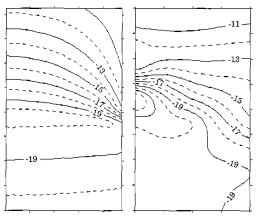

calculation experiment

(c) 6 hr.

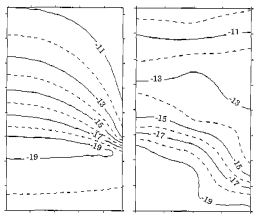

(d) 8 hr.

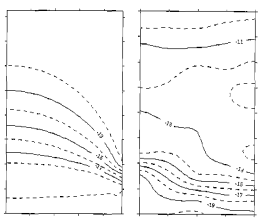

(e) 10 hr.

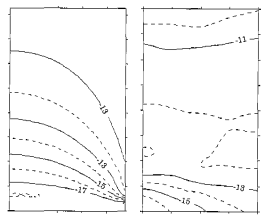

(f) 12 hr.

Fig. 11 The comparison of calculated and measured temperature distribution inside the drying material at 2, 4, 6, 8, 10, and 12 hours.

faster than that in the centerline.

In Fig. 11, the measured and calculated instantaneous temperature distributions inside a cylindrical container are presented at the interval of 2 hours. While the temperature field in the frozen region is almost 1-dimensional, that in the dried region shows much distortion by the heat transfer from the side-wall of the container. But as the thermal conductivity of the dried region is two orders of magnitude smaller than that of the frozen layer, the distortion of temperature distribution in the dried region does not have much effect on the deformation of the sublimation interface. From the figure, the numerical and experimental results agree well with each other in the configuration of isotherm and the temperature range in the domain. The curvature of isotherm in the dried region is larger in the experimental results than in the numerical results.

6. Conclusion.

A numerical program for the analysis of the freeze drying in a vial is developed based on a finite volume method with a moving grid system in this study and a freeze drying of skim milk in a vial is simulated with the program. From the simulation, the reduction of mass of drying material, the history and distribution of temperature and the evolution of the sublimation interface are obtained and presented. The calculated sublimation interface and temperature distribution demonstrates that the importance of considering the multi-dimensional effect for the accurate prediction of the freeze drying in a vial. From the simulation

results, it is assured if proper boundary conditions and material properties are provided the numerical program can produce accurate prediction of the process, and the present numerical procedure can be a useful tool for the analysis of freeze drying process in a vial.

REFERENCES

1) FERZIGER, J.H. AND PERIC, M. Computational Methods for Fluid Dynamics. Springer-Verlag, 1996.
2) KIM, C.-J. A Coordinate-Free Form of the Finite Gradient in Discretizing Scalar and Momentum Diffusion. In Proceedings of the 4th JSME-KSME Thermal Engineering Conference (Kobe, Japan, 2000).
3) LIAPIS, A.I. AND LITCHFIELD, R.J. Optimal Control of a Freeze Dryer. Chemical Engineering Science 34 (1979), 975-981.
4) LOMBRANA, J.I., ELVIRA, C.D. AND VILLARAN, M.C. Analysis of Operation Strategies in the Production of Special Foods in Vials by Freeze Drying. International Journal of Food and Technology 32 (1997), 107-115.
5) MASCARENHAS, W.J., AKAY, H.U. AND PIKAL, M.J. A Computational Model for Finite Element Analysis of the Freeze-Drying Process. Computer Methods in Applied Mechanics and Engineering 148 (1998), 105-124.
6) MILLMAN, M.J., LIAPIS, A.I. AND MARCHELLO, J.M. 1985, An Analysis of the Lyophilization Process using a Sorption-Sublimation Model and Various Operation Policies. AIChE Journal 31 (1985), 1594-1604.
7) SADIKOGLU, H. AND LIAPIS, A.I. Mathematical Modeling of the Primary and Secondary Drying Stages of Bulk Solution Freeze-Drying in Trays: Parameter Estimation and Model Discrimination by Comparison of Theoretical Results with Experimental Data. Drying Technology 15 (1997), 791-810.
8) SADIKOGLU, H., LIAPIS, A.I., CROSSER, O.K. AND BRUTTINI, R. Estimation of the effect of product shrinkage on the drying times, heat input and condenser load of the primary and secondary drying stages of the lyophilization process in vials. Drying Technology 17 (1999), 2013-2035.
9) SHEEHAN, P. AND LIAPIS, A.I. Modeling of the Primary and Secondary Drying Stages of the Freeze Drying of Pharmaceutical Products in Vials: Numerical Results obtained from the Solution of a Dynamic and Spatially Multi-Dimensional Lyophilization Model for Different Operation Policies. Biotechnology and Bioengineering 60 (1998), 712-728.
10) WANG, Z.H. AND SHI, M.H. The Effect of Sublimation-Condensation Region on Heat and Mass Transfer during Microwave Freeze Drying. Journal of Heat Transfer 120 (1998), 654-660.

저 자 소 개

송저설(宋致成)

1961년 4월 19일생. 1883년 한국해양대학 교기관학과 졸업. 1989년 동대학 대학원 기계공학과 졸업. 1996년 선박기계 기술사. 1989~현재 2001년 서울대학교 대학원 기계공학과졸업. 공학박사.